## Effect of Magnetic Impurities on Superfluid <sup>3</sup>He

A. M. Zimmerman<sup>®</sup>, M. D. Nguyen<sup>®</sup>, J. W. Scott<sup>®</sup>, and W. P. Halperin<sup>®</sup><sup>†</sup>
Northwestern University, Evanston, Illinois 60208, USA

(Received 16 August 2019; published 13 January 2020)

It is known that both magnetic and nonmagnetic impurities suppress unconventional superconductivity. Here we compare their effect on the paradigm unconventional superconductor, superfluid  ${}^{3}$ He, using highly dilute silica aerogel. Switching magnetic to nonmagnetic scattering in the same physical system is achieved by coating the aerogel surface with  ${}^{4}$ He. We find a marginal influence on the transition temperature itself. However, we have discovered that the A phase, which breaks time reversal symmetry, is strongly influenced, while the isotropic B phase is unchanged. Importantly, this occurs only if the impurities are anisotropically distributed on a global scale.

DOI: 10.1103/PhysRevLett.124.025302

Unlike conventional superconductors, unconventional superconductors are affected by the presence of both magnetic and nonmagnetic impurity scattering of quasiparticles. In fact the suppression of the superconducting transition by nonmagnetic impurities is generally considered to be an important indication of unconventional pairing. For example, there are equivalent effects on the transition temperature for substitution of either magnetic or nonmagnetic 4+ ions for ruthenium in the unconventional superconductor, Sr<sub>2</sub>RuO<sub>4</sub> [1], although its order parameter symmetry is in question [2]. A similar conclusion was drawn from impurity studies of the f-wave superconductor UPt<sub>3</sub> [3]. Extensive theoretical and experimental work on impurities in cuprates is reviewed by Balatsky et al. [4]. In particular, magnetic and nonmagnetic impurities can have different effects [5,6].

Superfluid <sup>3</sup>He is well established as an unconventional superfluid with *p*-wave, spin-triplet pairing. Recent experiments on <sup>3</sup>He confined in slabs or ordered aerogels show a significant difference between magnetic and nonmagnetic scattering both in the suppression of the superfluid transition and in the symmetry of the stable superfluid phases [7,8]. Here, we have carried out a systematic study comparing the effect of magnetic and nonmagnetic impurities on the superfluid phases using correlated point impurities from dilute silica aerogel. In contrast to previous studies we find the transition temperature to be relatively unaffected, but there is a significant effect on the stability of phases with different order parameter symmetry.

Pure <sup>3</sup>He has two superfluid states at low magnetic fields, each with unique symmetry: the isotropic, nonequal spin pairing (non-ESP) *B* phase and, above a pressure of 21 bar, the anisotropic, ESP *A* phase. Although <sup>3</sup>He is inherently pure, highly porous aerogel can be used to introduce impurity into the system [9]. Aerogels consist of correlated networks of small particles that act as impurities. Global anisotropy of the <sup>3</sup>He quasiparticle mean-free path results

from a preferred direction in the particle distributions, achieved by compression of isotropic aerogel, and plays a large role in the stability of phases with different order parameter symmetry [10–15]. Recent experiments have been conducted in highly anisotropic, nematically ordered alumina aerogels in which aerogel particles form parallel strands [7,13,14,16]. In the presence of these highly ordered impurities, new physical phenomena have been reported, including a new superfluid phase, the polar phase [14], and half-quantum vortices [15]. The pressure-temperature superfluid phase diagram in this system [7], as well as in thin slabs [8], appears to be greatly affected by magnetic scattering, raising the question of how different superfluid phases are affected by magnetic impurity. To answer this question, we have investigated the role of magnetic impurities on superfluid <sup>3</sup>He in anisotropic silica aerogels.

Aerogels used in experiments on superfluid <sup>3</sup>He are not intrinsically magnetic; however, a few layers of paramagnetic solid <sup>3</sup>He adsorbed on the surface creates a channel for magnetic quasiparticle scattering [17–20]. This paramagnetic solid can be removed by replacing the magnetic <sup>3</sup>He on the surface with nonmagnetic <sup>4</sup>He, allowing the switch from magnetic to nonmagnetic impurity. We note that the addition of <sup>4</sup>He also modifies the specularity of quasiparticle scattering, although this effect should be negligible at high pressures [21-24]. Dmitriev et al. [7] show that the newly observed polar phase is only present with nonmagnetic aerogel impurities. Additionally, the transition temperature,  $T_c$ , from the normal state to the superfluid was noticeably suppressed [7]. This effect was not observed in early experiments with isotropic silica aerogels [25,26].

Most theoretical work on superfluid <sup>3</sup>He has not addressed the effects of magnetic impurities [27–30], or focused on magnetic impurities in the absence of anisotropy [31–33]. New calculations, motivated by Ref. [7], indicate

that magnetic impurity might reduce the effects of anisotropy [34]. However other recent calculations find only small changes in the phase diagram due to magnetic scattering [35]. Clearly, more experimental work is needed.

We measured the pressure-temperature-field phase diagram of superfluid  ${}^{3}$ He with magnetic and nonmagnetic impurities using an aerogel sample with less anisotropy than alumina aerogels [7], and found that the phase diagram is significantly modified by magnetic impurity. In particular, the anisotropic A phase is suppressed by magnetic impurities while the isotropic B phase is unaffected. Unlike measurements in nematic aerogel, we do not observe large changes in  $T_c$ , Fig. 2, and Supplemental Material [36].

The sample used in our experiments is a 5.1-mm long, 4-mm diameter cylinder of 98% porous silica aerogel. Following growth and supercritical drying, anisotropy was induced by axial compression of the sample by 19.4%. It had been used previously to study the field-temperature phase diagram of superfluid <sup>3</sup>He in compressed aerogel with magnetic impurities at high pressure (26 bar) [11], as well as to study the orientation of the order parameter in the *B* phase [40]. Prior to compression, the same sample was studied in its isotropic state [41,42]. These experiments, carried out with magnetic impurity, provide a baseline for the comparison with nonmagnetic impurities that we report here.

In the present work, we performed measurements using pulsed nuclear magnetic resonance (NMR) in magnetic fields ranging from H = 49.1 to 196 mT with the field parallel to the aerogel anisotropy axis. The superfluid phases can be identified by the frequency shift,  $\Delta \omega$ , of the NMR resonance away from the Larmour frequency,  $\omega_L$ , as well as the magnetic susceptibility,  $\chi$ , which is proportional to the integral of the NMR spectrum.  $\Delta \omega$  determines longitudinal resonance frequency,  $\Omega$ , where  $\Delta\omega(T) \propto \Omega(T)^2$ , and  $\Omega$  is proportional to the amplitude of the order parameter  $\Delta$ . Measurements between 7.5 and 15 bar with magnetic impurities were taken to supplement earlier work at 26 bar [11,43]. Then, sufficient <sup>4</sup>He to replace the solid  ${}^{3}$ He on the surface,  $\sim 3.5$  layers, was mixed with <sup>3</sup>He at room temperature and introduced supercritically to the sample cell at T > 10 K. We verified the complete absence of solid <sup>3</sup>He on the aerogel surface using NMR. Measurements were conducted between 2.5 and 27 bar, during which the sample was warmed above 10 K several times. There was no evidence for damage to the aerogel as might be indicated by a change in the normal state line width, nominally 5 ppm, or any change in the superfluid phase diagram.

The most striking result of previous experiments on compressed silica aerogel with magnetic impurities is that the isotropic *B* phase appears to be more stable than the anisotropic *A* phase in a small magnetic field [11,43]. This is contrary to theoretical predictions [27,29,44], which show that anisotropic scattering should stabilize anisotropic

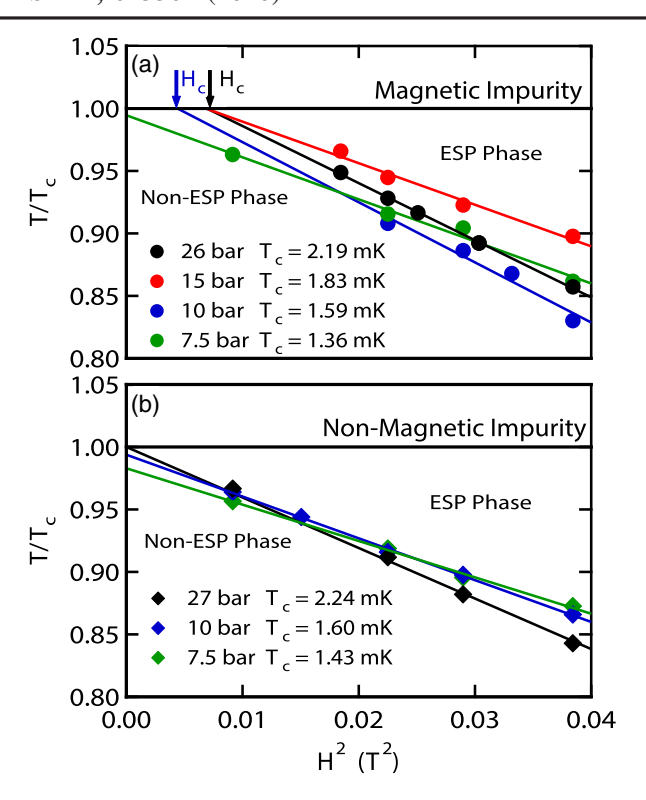


FIG. 1. The temperature-field superfluid phase diagram showing the dependence of  $T_{AB}/T_c$  on magnetic field at a variety of pressures.  $T_{AB}/T_c$  depends quadratically on magnetic field in all cases. (a) With magnetic impurities a critical field,  $H_c$ , is present at P=27 bar ( $H_c=88.6$  mT) 15 bar ( $H_c=82.6$  mT), and 10 bar ( $H_c=66.4$  mT), but is absent at lower pressure. (b) With nonmagnetic impurity  $H_c=0$ .

states. The phenomenon is manifest as a critical field,  $H_c$ , in the temperature-field phase diagram, Fig. 1(a).  $H_c$  occurs at the intersection of the quadratic field dependent transition between the ESP and non-ESP phases (A and B),  $T_{AB}(H^2)$ , with  $T_c$ . For an isotropic aerogel this intersection is precisely at H=0 [41,42].  $H_c$  was found to be proportional to anisotropy at P=26 bar [43].

In the present work, we find that removing the magnetic impurity eliminates  $H_c$ , Fig. 1(b). This shows it is the anisotropic distribution of magnetic impurities that gives rise to  $H_c$ , favoring the non-ESP phase over the ESP phase. Additionally, we extended measurements with magnetic impurities to lower pressure, finding that  $H_c$  decreases with decreasing pressure. It is essentially unmodified from 26 to 15 bar, reduced at 10 bar, and completely absent at 7.5 bar, Fig. 1(a). For the case of nonmagnetic impurities, at low pressure an anisotropic ESP phase appears in a small window of temperature below  $T_c$  in agreement with theoretical predictions [27,29,44].

To identify the ESP and non-ESP phases and determine how they are affected by magnetic impurities, we look at the frequency shift,  $\Delta\omega$ , of the NMR resonance in the superfluid state that is dependent on the specific superfluid state, the orientation of the order parameter, and the tipping

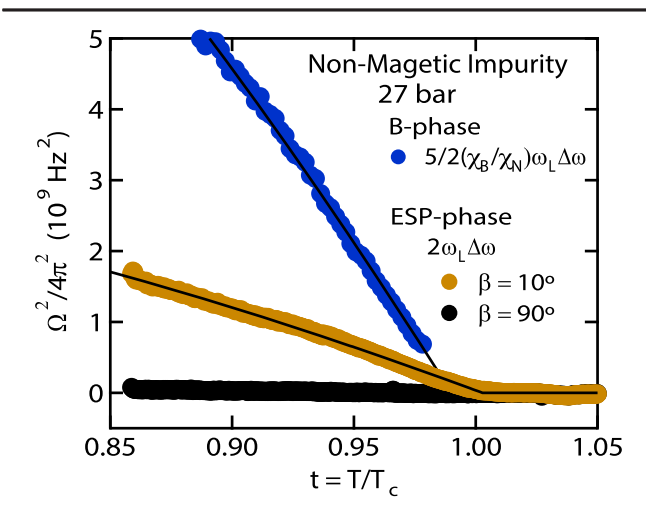


FIG. 2. Longitudinal resonance frequencies calculated from the NMR frequency shift at P=27 bar with nonmagnetic impurities, plotted versus reduced temperature,  $t=T/T_c$ . Data in the B phase were taken at a magnetic field of 0.1 T (blue circles) and data in the ESP phase at a magnetic field of 0.2 T (yellow circles). Black circles are calculated from the frequency shift measured after a 90° tip angle pulse in the ESP phase. The frequency shift is 0 at 90°, consistent with a polar phase or two-dimensional (2D)-disordered A phase. Solid lines are fits used to extract the initial slope, as described in the text.

angle,  $\beta$ , of the NMR pulse [9]. We measured  $\Delta\omega$  for the non-ESP phase with magnetic and nonmagnetic surface conditions and find that it has the same unique tip angle dependence as the B phase [40]. On this basis we identify the non-ESP phase as the B phase. At temperatures within 20% of  $T_c$  the angular momentum axis is perpendicular to the magnetic field resulting in a large frequency shift at small  $\beta$  from which the longitudinal resonance frequency can be determined by

$$\Omega_B^2(P,T) = \frac{5}{2}\omega_L\Delta\omega \qquad \beta \approx 0^{\circ}.$$
 (1)

This is shown in Fig. 2 where we have multiplied  $\Omega_B^2(P,T)$  by the magnetic susceptibility for later comparison with the ESP phase.

The B phase longitudinal resonance frequency is temperature dependent, so we characterize it by the initial slope of  $(\chi_B/\chi_N)\Omega_B^2$  relative to  $T/T_c$  as T approaches  $T_c$ , which we extract from a fit to the  $T/T_c$  dependence of the frequency shift measured in pure superfluid  $^3$ He [45,46]. Example fits are shown in Fig. 2. We denote this slope as  $\chi\Omega_{0B}^2 = d[(\chi_B/\chi_N)\Omega_B^2]/dt$ .  $\Omega_{0B}^2$  uniquely determines the longitudinal resonance frequency at all temperatures. As shown in Fig. 3(a), there is no discernible difference in the B phase longitudinal resonance frequency with magnetic or nonmagnetic scattering. We infer that the B phase order parameter is unaffected by the presence of magnetic impurities. Note that  $\chi\Omega_{0B}^2$  is linear in pressure. This linear

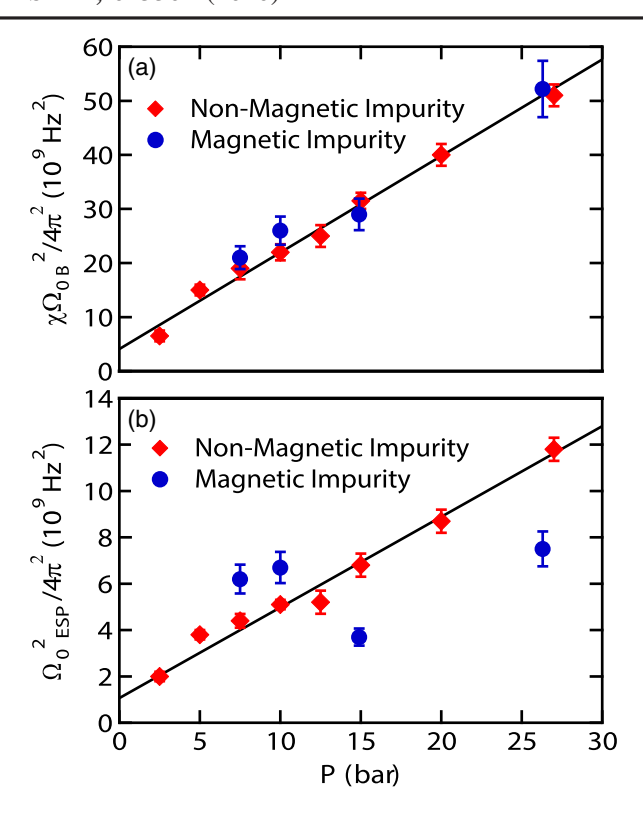


FIG. 3. Initial slope of the temperature dependent longitudinal resonance frequency,  $d\Omega^2/dt$ , as a function of pressure: (a) in the B phase, and (b) in the ESP phase. With nonmagnetic impurities (red diamonds), both phases have a linear pressure dependence, an important indication of a common superfluid state throughout the range of pressure. Changing from nonmagnetic to magnetic impurities (blue circles) has no effect on the values measured in the B phase, while the ESP phase is strongly affected. Error bars are from fits as shown in Fig. 2.

pressure dependence is observed in pure <sup>3</sup>He [45,47], isotropic aerogel [41], and anisotropic aerogel [10]. It is a ubiquitous property of superfluid <sup>3</sup>He phases [48], and it is a useful measure of the uniformity of the superfluid state as a function of pressure. We conclude that the non-ESP phase is the *B* phase at all pressures and is immune from magnetic impurity. Note that there is an increase in the longitudinal resonance frequency of the *B* phase relative to the same aerogel in its uncompressed state that is associated with global anisotropy [41].

The identification of the ESP phase is more complicated. At high pressure in the same sample, we identified the ESP phase in the presence of magnetic impurity as the A phase disordered into a 2D orbital glass, with its orbital angular momentum randomly oriented in the plane perpendicular to the aerogel anisotropy axis [42]. This 2D glass phase was also seen in alumina aerogel [14,49,50], and its presence suggests that the nature of disorder in axially compressed silica aerogel is the same as that of nematic aerogel. The other candidate for the ESP phase is the polar state. With magnetic field parallel to the aerogel anisotropy axis, both

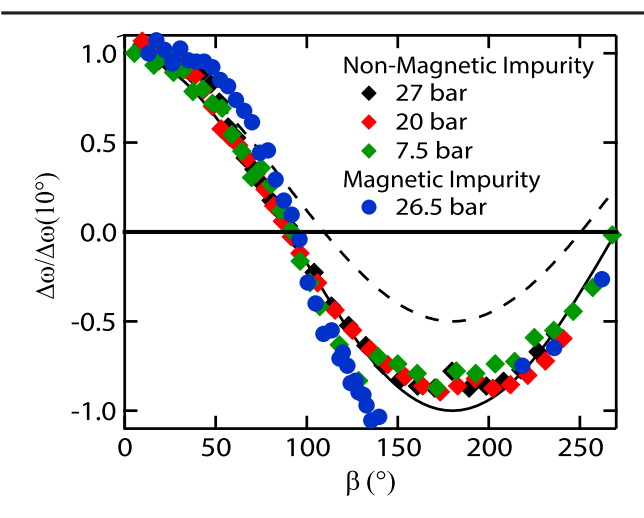


FIG. 4. Tip angle dependence of  $\Delta\omega$  in the ESP phase at several pressures, with both magnetic and nonmagnetic impurities. The solid curve is the calculated dependence for a polar phase or 2D-disordered *A* phase, while the dashed line is for an ordered *A* phase. In all cases the data agree with the solid curve.

of these phases have identical tip angle dependence, with frequency shift given by

$$2\omega_L \Delta \omega = \Omega_{\rm ESP}^2(P, T) \cos(\beta), \tag{2}$$

where  $\Omega^2_{\rm ESP}$  depends on the superfluid state of the ESP phase and is larger for the polar state than the A phase [14,48]. At all pressures and impurities, the frequency shift in the ESP phase follows this behavior, Fig. 4, and the tip angle dependence alone does not allow discrimination between the two possible states.

Following the same procedure used for the B phase, we extract the initial slope of  $\Omega^2_{\text{ESP}}$ , which we denote as  $\Omega_{0\,\mathrm{ESP}}^2 = d(\Omega_{\mathrm{ESP}}^2)/dt$ , Fig. 3. With nonmagnetic impurities,  $\Omega_{0 \, \text{ESP}}^2$  is linear in pressure, indicating that there is a single well-defined superfluid state throughout the whole pressure range. In contrast, with magnetic impurities,  $\Omega_{0 \, \text{ESP}}^2$  is nonlinear in pressure. At high pressure,  $\Omega_{0 \, \text{ESP}}^2$  is reduced by a factor of  $\sim 1.5$  compared to the value with nonmagnetic impurities, implying that the ESP phase is suppressed by magnetic impurities at these pressures. At low pressure  $\Omega_{0ESP}^2$  is slightly larger than the value measured with nonmagnetic impurities. We note that the transition between these two regions occurs between 10 and 15 bar, the same region where the critical field begins to decrease, Fig. 1. This change in behavior indicates that the ESP phase with magnetic impurities is a modified, or a different, superfluid state at low pressures. In either case, the results show that the ESP phase is strongly affected by magnetic impurity.

Identification of the ESP phase requires a comparison of  $\Omega^2_{0\, \rm ESP}$  with a known value as a reference. We use  $\Omega^2_B$  measured in our aerogel sample. The ratio of longitudinal

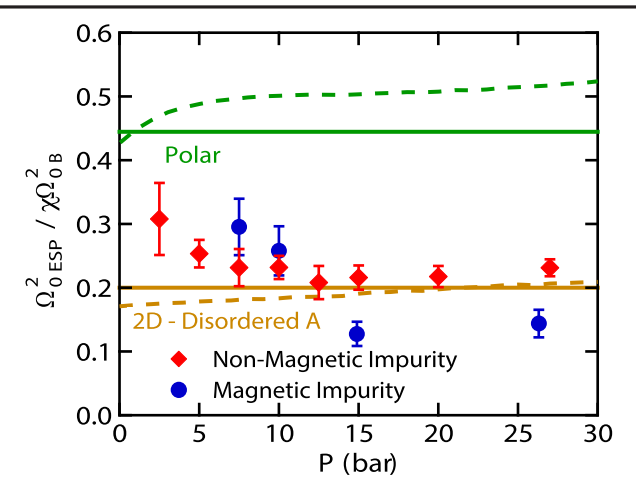


FIG. 5.  $\Omega_{0\,\mathrm{ESP}}^2/\chi\Omega_{0B}^2$  as a function of pressure with magnetic impurities (blue circles) and with nonmagnetic impurities (red diamonds). Solid lines are the theoretical ratios discussed in the text between the 2D-disordered A phase and B phase (yellow), and the polar phase and B phase (green), while dashed lines are calculated from the pure <sup>3</sup>He Ginzburg-Landau theory. At all pressures the data are more consistent with the 2D-disordered A phase, although the increase at low pressures may be due to polar distortion. Error bars are calculated from the errors in  $\Omega_{0\,\mathrm{ESP}}^2$  and  $\chi\Omega_{0B}^2$ .

resonance frequencies of different phases is determined by the symmetry of those phases, and comparison with the B phase has previously been used to identify the ESP phase as the A phase in pure  ${}^{3}$ He [51,52], as well as in isotropic aerogel [41]. We have calculated the ratio from our experimental values as  $\Omega_{0ESP}^{2}/\chi\Omega_{0B}^{2}$ , as shown in Fig. 5.

For the 2D-disordered *A* phase, the ratio with the *B* phase longitudinal resonance frequency is given by

$$\frac{\chi_N \Omega_A^2}{\chi_B \Omega_B^2} = \frac{1}{5} \left( \frac{\Delta_A}{\Delta_B} \right)^2, \tag{3}$$

where  $\Delta$  is the average amplitude of the order parameter [48,53]. We can take  $\Delta_A/\Delta_B \approx 1$  [41,51]. Similarly, for the polar phase, we have

$$\frac{\chi_N \Omega_P^2}{\chi_B \Omega_R^2} = \frac{4}{5} \left(\frac{\Delta_P}{\Delta_B}\right)^2,\tag{4}$$

where we can use the low pressure, weak coupling value of  $((\Delta_P/\Delta_B)^2 = 5/9$  [48]. These calculated ratios are shown as solid lines in Fig. 5. Alternatively,  $\Delta$  can be calculated from the experimental pure <sup>3</sup>He Ginzburg-Landau parameters [54] shown by the dashed lines in Fig. 5.

Without magnetic impurities, at high pressure, the experimental values of  $\Omega_{0\,\text{ESP}}^2/\chi\Omega_{0B}^2$  are consistent with the 2D-disordered *A* phase and rule out the polar state. With magnetic impurities neither ratio is correct, indicating that the suppression of the *A* phase distorts its order parameter,

changing the relative symmetry compared to the B phase. At low pressure, both with and without magnetic impurities,  $\Omega_{0\,\mathrm{ESP}}^2/\chi\Omega_{0B}^2$  is larger than expected for the A phase, though not as large as for the polar phase. This may be due to polar distortion of the A phase at low pressures, or a change in the A phase itself. In either case this identification shows that the A phase is affected by magnetic impurities, in contrast to previous work where only the polar phase was shown to be affected [7].

In summary, we find a significant effect of magnetic impurity suppression of the superfluid *A* phase, the phase that breaks time reversal symmetry. In contrast the time reversal symmetric *B* phase is unaffected. The existence of a critical field that was reported previously [11,43] can be entirely attributed to anisotropic magnetic quasiparticle scattering. Finally, the transition temperature is only weakly affected. Our work extends the model system of superfluid <sup>3</sup>He as a paradigm for understanding other unconventional superconductors, where magnetic quasiparticle scattering may play an essential role in determining the symmetry of the order parameter.

We are grateful to J. A. Sauls, J. J. Wiman, V. V. Dmitriev, and G. E. Volovik for helpful discussion, and support from the National Science Foundation (Grant No. DMR-1903053).

- \*andrewzimmerman2016@u.northwestern.edu
  †w-halperin@northwestern.edu
- N. Kikugawa, A. Peter Mackenzie, and Y. Maeno, J. Phys. Soc. Jpn. 72, 237 (2003).
- [2] A. Pustogow, Y. Luo, A. Chronister, Y.-S. Su, D. A. Sokolov, F. Jerzembeck, A. P. Mackenzie, C. W. Hicks, N. Kikugawa, S. Raghu, E. D. Bauer, and S. E. Brown, Nature (London) 574, 72 (2019).
- [3] Y. Dalichaouch, M. C. de Andrade, D. A. Gajewski, R. Chau, P. Visani, and M. B. Maple, Phys. Rev. Lett. 75, 3938 (1995).
- [4] A. V. Balatsky, I. Vekhter, and J.-X. Zhu, Rev. Mod. Phys. 78, 373 (2006).
- [5] E. W. Hudson, K. M. Lang, V. Madhavan, S. H. Pan, H. Eisaki, S. Uchida, and J. C. Davis, Nature (London) 411, 920 (2001).
- [6] P. Monthoux and D. Pines, Phys. Rev. B 49, 4261 (1994).
- [7] V. V. Dmitriev, A. A. Soldatov, and A. N. Yudin, Phys. Rev. Lett. 120, 075301 (2018).
- [8] P. J. Heikkinen, A. Casey, L. V. Levitin, X. Rojas, A. Vorontsov, P. Sharma, N. Zhelev, J. M. Parpia, and J. Saunders, arXiv:1909.04210.
- [9] W. Halperin, Annu. Rev. Condens. Matter Phys. 10, 155 (2019).
- [10] J. Pollanen, J. I. A. Li, C. A. Collett, W. J. Gannon, W. P. Halperin, and J. A. Sauls, Nat. Phys. 8, 317 (2012).
- [11] J. I. A. Li, A. M. Zimmerman, J. Pollanen, C. A. Collett, W. J. Gannon, and W. P. Halperin, Phys. Rev. Lett. 112, 115303 (2014).

- [12] N. Zhelev, M. Reichl, T. Abhilash, E. Smith, K. Nguyen, E. Mueller, and J. Parpia, Nat. Commun. 7, 12975 (2016).
- [13] V. E. Asadchikov, R. S. Askhadullin, V. V. Volkov, V. V. Dmitriev, N. K. Kitaeva, P. N. Martynov, A. A. Osipov, A. A. Senin, A. A. Soldatov, D. I. Chekrygina, and A. N. Yudin, JETP Lett. 101, 556 (2015).
- [14] V. V. Dmitriev, A. A. Senin, A. A. Soldatov, and A. N. Yudin, Phys. Rev. Lett. 115, 165304 (2015).
- [15] S. Autti, V. V. Dmitriev, J. T. Makinen, A. A. Soldatov, G. E. Volovik, A. N. Yudin, V. V. Zavjalov, and V. B. Eltsov, Phys. Rev. Lett. 117, 255301 (2016).
- [16] V. V. Dmitriev, L. A. Melnikovsky, A. A. Senin, A. A. Soldatov, and A. N. Yudin, JETP Lett. 101, 808 (2015).
- [17] J. A. Sauls, Y. M. Bunkov, E. Collin, H. Godfrin, and P. Sharma, Phys. Rev. B 72, 024507 (2005).
- [18] E. Collin, S. Triqueneaux, Y. M. Bunkov, and H. Godfrin, Phys. Rev. B 80, 094422 (2009).
- [19] A. Schuhl, S. Maegawa, M. W. Meisel, and M. Chapellier, Phys. Rev. B 36, 6811 (1987).
- [20] D. I. Bradley, S. N. Fisher, A. M. Guénault, R. P. Haley, N. Mulders, G. R. Pickett, D. Potts, P. Skyba, J. Smith, V. Tsepelin, and R. C. V. Whitehead, Phys. Rev. Lett. 105, 125303 (2010).
- [21] M. R. Freeman and R. C. Richardson, Phys. Rev. B 41, 11011 (1990).
- [22] S. M. Tholen and J. M. Parpia, Phys. Rev. Lett. 67, 334 (1991).
- [23] S. B. Kim, J. Ma, and M. H. W. Chan, Phys. Rev. Lett. 71, 2268 (1993).
- [24] S. Murakawa, M. Wasai, K. Akiyama, Y. Wada, Y. Tamura, R. Nomura, and Y. Okuda, Phys. Rev. Lett. 108, 025302 (2012)
- [25] V. V. Dmitriev, I. V. Kosarev, N. Mulders, V. V. Zavjalov, and D. Y. Zmeev, Physica (Amsterdam) 329B–333B, 320 (2003)
- [26] D. T. Sprague, T. M. Haard, J. B. Kycia, M. R. Rand, Y. Lee, P. J. Hamot, and W. P. Halperin, Phys. Rev. Lett. 77, 4568 (1996).
- [27] E. V. Thuneberg, S. K. Yip, M. Fogelström, and J. A. Sauls, Phys. Rev. Lett. 80, 2861 (1998).
- [28] J. A. Sauls, Phys. Rev. B 88, 214503 (2013).
- [29] K. Aoyama and R. Ikeda, Phys. Rev. B **73**, 060504(R) (2006).
- [30] K. Aoyama and R. Ikeda, Phys. Rev. B 72, 012515 (2005).
- [31] J. A. Sauls and P. Sharma, Phys. Rev. B 68, 224502 (2003).
- [32] G. Baramidze and G. Kharadze, Physica (Amsterdam) **284B–288B**, 305 (2000).
- [33] R. Ikeda and K. Aoyama, Phys. Rev. B 79, 064527 (2009).
- [34] V. P. Mineev, Phys. Rev. B 98, 014501 (2018).
- [35] I. A. Fomin, JETP 127, 933 (2018).
- [36] See Supplemental Material at http://link.aps.org/supplemental/ 10.1103/PhysRevLett.124.025302 for additional information on changes in the transition temperature, which includes Refs. [7,31,37–40].
- [37] A. A. Abrikosov and L. P. Gorkov, J. Exp. Theor. Phys. 15, 752 (1962).
- [38] A. I. Larkin, JETP Lett. 2, 130 (1965).
- [39] I. A. Fomin, JETP Lett. 88, 59 (2008).
- [40] A. M. Zimmerman, J. I. A. Li, M. D. Nguyen, and W. P. Halperin, Phys. Rev. Lett. 121, 255303 (2018).

- [41] J. Pollanen, J. I. A. Li, C. A. Collett, W. J. Gannon, and W. P. Halperin, Phys. Rev. Lett. 107, 195301 (2011).
- [42] J.I.A. Li, J. Pollanen, A.M. Zimmerman, C.A. Collett, W.J. Gannon, and W.P. Halperin, Nat. Phys. 9, 775 (2013).
- [43] J. I. A. Li, A. M. Zimmerman, J. Pollanen, C. A. Collett, and W. P. Halperin, Phys. Rev. Lett. 114, 105302 (2015).
- [44] C. L. Vicente, H. C. Choi, J. S. Xia, W. P. Halperin, N. Mulders, and Y. Lee, Phys. Rev. B 72, 094519 (2005).
- [45] P. E. Schiffer, Studies of the superfluid phases of helium three and the magnetization of thin solid films of helium three, Ph. D. thesis, Stanford University, 1993.
- [46] P. Schiffer, M. T. O'Keefe, H. Fukuyama, and D. D. Osheroff, Phys. Rev. Lett. 69, 3096 (1992).
- [47] M. R. Rand et al., Phys. Rev. Lett. 77, 1314 (1996).

- [48] A. M. Zimmerman, M. D. Nguyen, and W. P. Halperin, J. Low Temp. Phys. 195, 358 (2019).
- [49] R. S. Askhadullin, V. V. Dmitriev, D. A. Krasnikhin, P. N. Martinov, A. A. Osipov, A. A. Senin, and A. N. Yudin, JETP Lett. 95, 326 (2012).
- [50] R. S. Askhadullin, V. V. Dmitriev, P. N. Martynov, A. A. Osipov, A. A. Senin, and A. N. Yudin, JETP Lett. 100, 662 (2015).
- [51] D. D. Osheroff, Phys. Rev. Lett. 33, 1009 (1974).
- [52] M. R. Rand, H. H. Hensley, J. B. Kycia, T. M. Haard, Y. Lee, P. J. Hamot, and W. P. Halperin, Physica (Amsterdam) 194B, 805 (1994).
- [53] A. J. Leggett, Rev. Mod. Phys. 47, 331 (1975).
- [54] H. Choi, J. P. Davis, J. Pollanen, T. M. Haard, and W. P. Halperin, Phys. Rev. B 75, 174503 (2007).